

The Status and future of ground-based TeV gamma-ray astronomy

Reports of Individual Working Groups

1 Gamma-ray bursts

Group membership:

A. D. Falcone, D. A. Williams, M. G. Baring, R. Blandford, J. Buckley, V. Connaughton, P. Coppi, C. Dermer, B. Dingus, C. Fryer, N. Gehrels, J. Granot, D. Horan, J. I. Katz, K. Kuehn, P. Mészáros, J. Norris, P. Saz Parkinson, A. Pe’er, E. Ramirez-Ruiz, S. Razzaque, X.-Y. Wang, and B. Zhang

1.1 Introduction

High energy astrophysics is a young and relatively undeveloped field, which owns much of the unexplored “discovery space” in contemporary astronomy. The edge of this discovery space has recently been illuminated by the current generation of very high energy (VHE) telescopes, which have discovered a diverse catalog of more than seventy VHE sources. At this time, gamma ray bursts (GRBs) have eluded attempts to detect them with VHE telescopes (although some tentative, low-significance detections have been reported). However, theoretical predictions place them near the sensitivity limits of current instruments. The time is therefore at hand to increase VHE telescope sensitivity, thus facilitating the detection of these extreme and mysterious objects.

Much has been learned since the discovery of GRBs in the late 1960s. There are at least two classes of GRB, most conveniently referred to as “long” and “short,” based on the duration and spectral hardness of their prompt sub-MeV emission. The distribution of the types and star for-

mation rates of the host galaxies suggests different progenitors for these two classes. The exact nature of the progenitors nevertheless remains unknown, although it is widely believed that long GRBs come from the deaths of massive rotating stars and short GRBs result from compact object mergers. The unambiguous solution to this mystery is critical to astrophysics since it has fundamental importance to several topics, including stellar formation history and ultra high energy cosmic ray acceleration. A detection of VHE emission from GRBs would severely constrain the physical parameters surrounding the particle acceleration from GRBs and the energy injected into the particle acceleration sites, and would therefore constrain the properties of the GRB progenitors themselves. These same observations would constrain models for cosmic ray acceleration.

One of the big questions regarding GRBs is whether the jets are dominated by ultrarelativistic protons, that interact with either the radiation field or the background plasma, or are dominated by e^+e^- pairs. The combination of Fermi and current generation VHE telescopes such as HESS, MAGIC and VERITAS will contribute to progress on these questions in the near term, but more sensitive observations will likely be needed.

The same shocks which are thought to accelerate electrons responsible for non-thermal γ -rays in GRBs should also accelerate protons. Both the internal and the external reverse shocks are expected to be mildly relativistic, and are expected to lead to relativistic protons. The maximum proton energies achievable in GRB shocks are estimated to be $\sim 10^{20}$ eV, comparable to the highest energies of the mysterious ultra high en-

ergy cosmic rays measured with large ground arrays. The accelerated protons can interact with the fireball photons, leading to pions, followed by high-energy gamma rays, muons, and neutrinos. Photopion production is enhanced in conditions of high internal photon target density, whereas if the density of (higher-energy) photons is too large, the fireball is optically thick to gamma-rays, even in a purely leptonic outflow. High-energy gamma-ray studies of GRBs provide a direct probe of the shock proton acceleration as well as of the photon density.

1.1.1 Status of theory on emission models

Gamma-ray burst νF_ν spectra have a peak at photon energies ranging from a few keV to several MeV, and the spectra are nonthermal. From EGRET data, it is clear that the spectra extend to at least several GeV [1, 2, 3, 4], and there is a possible detection in the TeV range by Milagro [5, 6]. These non-thermal spectra imply that a significant fraction of the explosion energy is first converted into another form of energy before being dissipated and converted to nonthermal radiation. The most widely accepted interpretation is the conversion of the explosion energy into kinetic energy of a relativistic flow [7, 8, 9]. At a second stage, the kinetic energy is converted into radiation via internal collisions (internal shock model) resulting from variability in the ejection from the progenitor [10, 11] or an external collision (external shock model) with the surrounding medium [12, 13, 14]. The collisions produce shock waves, which enhance and are believed to create magnetic fields, as well as to accelerate electrons to high energies [15, 16, 17, 18, 19]. In the standard theoretical model, the initial burst of emission described above (prompt emission) is followed by afterglow emission, discussed below, from an external shock that moves through the circumburst environment.

Flux variability in GRBs is seen on timescales as short as milliseconds and can occur at late times. This rapid variability can be easily explained in the internal shock model, which makes it the

most widely used model. It can also be explained in the context of the external shock model either if one assumes variations in the strength of the magnetic field or in the energy transfer to the non-thermal electrons [20], or by collisions of the outflow with small, high density clouds in the surrounding medium [13, 14].

An alternative way of producing the emission involves conversion of the explosion energy into magnetic energy [21, 22, 23], which produces a flow that is Poynting-flux dominated. The emission is produced following dissipation of the magnetic energy via reconnection of the magnetic field lines [24, 25, 26, 27]. An apparent advantage of this model over the internal or external shock model is that the conversion of energy to radiation is much more efficient (see [28, 29] on the efficiency problem in the internal shocks model). The microphysics of the reconnection process in this model, like the microphysics determining the fraction of energy in relativistic electrons and in the magnetic field in the internal and external shock scenarios, is not yet fully understood.

VHE observations probe the extremes of the efficiency of energy conversion for each of these models and simultaneously probe the environment where the emission originated.

The dissipation of kinetic and/or magnetic energy leads to the emission of radiation. The leading emission mechanism employed to interpret the GRB prompt emission in the keV-MeV region of the spectral energy distribution is non-thermal synchrotron radiation [30, 31, 32]. An order of magnitude estimate of the maximum observed energy of photons produced by synchrotron emission was derived in [33]: Assuming that the electrons are Fermi accelerated in the shock waves, the maximum Lorentz factor of the accelerated electrons γ_{\max} is found by equating the particle acceleration time and the synchrotron cooling time, yielding $\gamma_{\max} = 10^5/\sqrt{B/10^6}$, where B is the magnetic field strength in gauss. For relativistic motion with bulk Lorentz factor Γ at redshift z , synchrotron emission from electrons with γ_{\max} peaks in the observer's frame at energy $70(\Gamma/315)(1+z)^{-1}$

GeV, which is independent of the magnetic field. Thus, synchrotron emission can produce photons with energies up to, and possibly exceeding, ~ 100 GeV.

Many of the observed GRB spectra were found to be consistent with the synchrotron emission interpretation [34, 35, 36]. However, a significant fraction of the observed spectra were found to be too hard (spectral photon index harder than $2/3$ at low energies) to be accounted for by this model [37, 38, 39, 40, 41]. This motivated studies of magnetic field tangling on very short spatial scales [42], anisotropies in the electron pitch angle distributions [43, 44], reprocessing of radiation by an optically thick cloud heated by the impinging gamma rays [45] or by synchrotron self absorption [46], and the contribution of a photospheric (thermal) component [47, 48, 49]. A thermal component that accompanies the first stages of the overall non-thermal emission and decays after a few seconds was consistent with some observations [50, 51]. Besides explaining the hard spectra observed in some of the GRBs seen by the Burst and Transient Source Experiment (BATSE), the thermal component provides seed photons that can be Compton scattered by relativistic electrons, resulting in a potential VHE gamma ray emission signature that can be tested.

A natural emission mechanism that can contribute to emission at high energies (\gtrsim MeV) is inverse-Compton (IC) scattering. The seed photons for the scattering can be synchrotron photons emitted by the same electrons, namely synchrotron self-Compton (SSC) emission [52, 53, 54, 55, 56, 57, 58, 59], although in some situations this generates MeV-band peaks broader than those observed [60]. The seed photons can also be thermal emission originating from the photosphere [61, 62], an accretion disk [63], an accompanying supernova remnant [64, 65], or supernova emissions in two-step collapse scenarios [66]. Compton scattering of photons can produce emission up to observed energies $15(\gamma_{\max}/10^5)(\Gamma/315)(1+z)^{-1}$ TeV, well into the VHE regime.

The shapes of the Comptonized emission spec-

tra in GRBs depend on the spectra of the seed photons and the energy and pitch-angle distributions of the electrons. A thermal population of electrons can inverse-Compton scatter seed thermal photons [67] or photons at energies below the synchrotron self-absorption frequency to produce the observed peak at sub-MeV energies [68]. Since the electrons cool by the IC process, a variety of spectra can be obtained [33, 62]. Comptonization can produce a dominant high-energy component [69] that can explain hard high-energy spectral components, such as that observed in GRB 941017 [4, 70, 71]. Prolonged higher energy emission could potentially be observed with a sensitive VHE gamma ray instrument.

The maximum observed photon energy from GRBs is limited by the annihilation of gamma rays with target photons, both extragalactic IR background and photons local to the GRB, to produce electron-positron pairs. This limit is sensitive to the uncertain value of the bulk motion Lorentz factor as well as to the spectrum at low energies, and is typically in the sub-TeV regime. Generally, escape of high-energy photons requires large Lorentz factors. In fact, observations of GeV photons have been used to constrain the minimum Lorentz factor of the bulk motion of the flow [72, 73, 74, 75, 76, 77], and spectral coverage up to TeV energies could further constrain the Lorentz factor [78, 79, 80]. If the Lorentz factor can be determined independently, e.g. from afterglow modeling, then the annihilation signature can be used to diagnose the gamma-ray emission region [81].

The evidence for acceleration of leptons in GRB blast waves is based on fitting lepton synchrotron spectra models to GRB spectra. This consistency of leptonic models with observed spectra still allows the possibility of hadronic components in these bursts, and perhaps more importantly, GRBs with higher energy emission have not been explored for such hadronic components due to the lack of sensitive instruments in the GeV/TeV energy range. The crucially important high-energy emission components, represented by only 5 EGRET spark chamber bursts,

a handful of BATSE and EGRET/TASC GRBs, and a marginal significance Milagro TeV detection, were statistically inadequate to look for correlations between high-energy and keV/MeV emission that can be attributed to a particular process. Indeed, the prolonged high-energy components in GRB 940217 and the “superbowl” burst, GRB 930131, and the anomalous gamma-ray emission component in GRB 941017, behave quite differently than the measured low-energy gamma-ray light curves. Therefore, it is quite plausible that hadronic emission components are found in the high energy spectra of GRBs.

Several theoretical mechanisms exist for hadronic VHE emission components. Accelerated protons can emit synchrotron radiation in the GeV–TeV energy band [82, 83, 84]. The power emitted by a particle is $\propto \gamma^2/m^2$, where γ is the Lorentz factor of the particle and m is its mass. Given the larger mass of the proton, to achieve the same output luminosity, the protons have ~ 1836 times higher mean Lorentz factor, the acceleration mechanism must convert ~ 3 million times more energy to protons than electrons and the peak of the proton emission would be at $\gtrsim 2000$ times higher energy than the peak energy of photons emitted by the electrons. Alternatively, high-energy baryons can produce energetic pions, via photomeson interactions with the low energy photons, creating high-energy photons and neutrinos following the pion decay [83, 85, 86, 87, 88, 89]. This process could be the primary source of ultra high energy (UHE) neutrinos. Correlations between gamma-ray opacity, bulk Lorentz factor, and neutrino production will test whether GRBs are UHE cosmic ray sources [90]. If the neutrino production is too weak to be detected, then the former two measurements can be obtained independently with sensitive GeV–TeV γ -ray telescopes and combined to test for UHE cosmic ray production. Finally, proton-proton or proton-neutron collisions may also be a source of pions [10, 91, 92, 93, 94], and in addition, if there are neutrons in the flow, then the neutron β -decay has a drag effect on the protons, which may produce another source of radiation [95].

Each of these cases has a VHE spectral shape and intensity that can be studied coupled with the emission measured at lower energies and with neutrino measurements.

Afterglow emission is explained in synchrotron-shock models by the same processes that occur during the prompt phase. The key difference is that the afterglow emission originates from large radii, $\gtrsim 10^{17}$ cm, as opposed to the much smaller radius of the flow during the prompt emission phase, $\simeq 10^{12} - 10^{14}$ cm for internal shocks, and $\simeq 10^{14} - 10^{16}$ cm for external shocks. As a result, the density of the blast-wave shell material is smaller during the afterglow emission phase than in the prompt phase, and some of the radiative mechanisms, e.g. thermal collision processes, may become less important.

Breaks in the observed lightcurves, abrupt changes in the power law slope, are attributed to a variety of phenomena, such as refreshed shocks originating from late time central engine activity [96, 97], aspherical variations in the energy [98], or variations in the external density [99, 100]. Blast wave energy escaping in the form of UHE neutrals and cosmic rays can also produce a rapid decay in the X-ray light curve [14]. In addition, interaction of the blast wave with the wind termination shock of the progenitor may be the source of a jump in the lightcurve [101, 102, 103], although this bump may not be present at a significant level [104]. High-energy gamma-ray observations may show whether new photohadronic emission mechanisms are required, or if the breaks do not require new radiation mechanisms for explanation (see, e.g., [105, 106]).

1.1.2 GRB Progenitors

We still do not know the exact progenitors of GRBs, and it is therefore difficult, if not impossible, to understand the cause of these cosmic explosions. These GRB sources involve emission of energies that can exceed 10^{50} ergs. The seat of this activity is extraordinarily compact, as indicated by rapid variability of the radiation flux on time scales as short as milliseconds. It is unlikely that mass can be converted into energy with bet-

ter than a few (up to ten) percent efficiency; therefore, the more powerful short GRB sources must “process” upwards of $10^{-3}M_{\odot}$ through a region which is not much larger than the size of a neutron star (NS) or a stellar mass black hole (BH). No other entity can convert mass to energy with such a high efficiency, or within such a small volume. The leading contender for the production of the longer class of GRBs — supported by observations of supernovae associated with several bursts — is the catastrophic collapse of massive, rapidly rotating stars. The current preferred model for short bursts, the merger of binary systems of compact objects, such as double neutron star systems (e.g. Hulse-Taylor pulsar systems) is less well established. A fundamental problem posed by GRB sources is how to generate over 10^{50} erg in the burst nucleus and channel it into collimated relativistic plasma jets.

The progenitors of GRBs are essentially masked by the resulting fireball, which reveals little more than the basic energetics and microphysical parameters of relativistic shocks. Although long and short bursts most likely have different progenitors, the observed radiation is very similar. Progress in understanding the progenitors can come from determining the burst environment, the kinetic energy and Lorentz factor of the ejecta, the duration of the central engine activity, and the redshift distribution. VHE gamma-ray observations can play a supporting role in this work. To the extent that we understand GRB emission across the electromagnetic spectrum, we can look for the imprint of the burst environment or absorption by the extragalactic background light on the spectrum as an indirect probe of the environment and distance, respectively. VHE emission may also prove to be crucial to the energy budget of many bursts, thus constraining the progenitor.

1.2 High-energy observations of gamma-ray bursts

Some of the most significant advances in GRB research have come from GRB correlative observa-

tions at longer wavelengths. Data on correlative observations at shorter wavelengths are sparse but tantalizing and inherently very important. One definitive observation of the prompt or afterglow emission could significantly influence our understanding of the processes at work in GRB emission and its aftermath. Although many authors have predicted its existence, the predictions are near or below the sensitivity of current instruments, and there has been no definitive detection of VHE emission from a GRB either during the prompt phase or at any time during the multi-component afterglow.

For the observation of photons of energies above 300 GeV, only ground-based telescopes are available. These ground-based telescopes fall into two broad categories, air shower arrays and imaging atmospheric Cherenkov telescopes (IACTs). The air shower arrays, which have wide fields of view that are suitable for GRB searches, are relatively insensitive. There are several reports from these instruments of possible TeV emission: emission >16 TeV from GRB 920925c [107], an indication of 10 TeV emission in a stacked analysis of 57 bursts [108], and an excess gamma-ray signal during the prompt phase of GRB 970417a [5]. In all of these cases however, the statistical significance of the detection is not high enough to be conclusive. In addition to searching the Milagro data for VHE counterparts for over 100 satellite-triggered GRBs since 2000 [109, 110, 111], the Milagro Collaboration conducted a search for VHE transients of 40 seconds to 3 hours duration in the northern sky [112]; no evidence for VHE emission was found from these searches.

IACTs have better flux sensitivity and energy resolution than air shower arrays, but are limited by their small fields of view ($3-5^{\circ}$) and low duty cycle ($\sim 10\%$). In the BATSE [113] era (1991–2000), attempts at GRB monitoring were limited by slew times and uncertainty in the GRB source position [114]. More recently, VHE upper limits from 20% to 62% of the Crab flux at late times ($\gtrsim 4$ hours) were obtained with Whipple Telescope for seven GRBs in 2002-2004 [115]. The MAGIC Collaboration took observa-

tions of GRB 050713a beginning 40 seconds after the prompt emission but saw no evidence for VHE emission [116]. Follow-up GRB observations have been made on many more GRBs by the MAGIC Collaboration [117] but no detections have been made [118, 119]. Upper limits of 2–7% of the Crab flux on the VHE emission following three GRBs have also been obtained with VERITAS [120].

One of the main obstacles for VHE observations of GRBs is the distance scale. Pair production interactions of gamma rays with the infrared photons of the extragalactic background light attenuate the gamma-ray signal, limiting the distance over which VHE gamma rays can propagate. The MAGIC Collaboration has reported the detection of 3C279, at redshift of 0.536 [121]. This represents a large increase in distance to the furthest detected VHE source, revealing more of the universe to be visible to VHE astronomers than was previously thought.

1.3 High Energy Emission Predictions for Long Bursts

As described earlier, long duration GRBs are generally believed to be associated with core collapses of massive rotating stars [122, 123], which lead to particle acceleration by relativistic internal shocks in jets. The isotropic-equivalent gamma-ray luminosity can vary from 10^{47} erg s $^{-1}$ all the way to 10^{53} erg s $^{-1}$. They are distributed in a wide redshift range (from 0.0085 for GRB 980425 [124] to 6.29 for GRB 050904 [125], with a mean redshift of 2.3–2.7 for Swift bursts, e.g. [126, 127]). The low redshift long GRBs ($z \lesssim 0.1$, e.g. GRB 060218, $z = 0.033$ [128]) are typically sub-luminous with luminosities of $10^{47} - 10^{49}$ erg s $^{-1}$ and spectral peaks at lower energies, so they are less likely detected at high energy. However, one nearby, “normal” long GRB has been detected (GRB 030329, $z = 0.168$), which has large fluences in both its prompt gamma-ray emission and afterglow.

1.3.1 Prompt emission

The leading model of the GRB prompt emission is the internal shock model [11], and we begin by discussing prompt emission in that context. The relative importance of the leptonic vs. hadronic components for high energy photon emission depends on the unknown shock equipartition parameters, usually denoted as ϵ_e , ϵ_B and ϵ_p for the energy fractions carried by electrons, magnetic fields, and protons, respectively. Since electrons are much more efficient emitters than protons, the leptonic emission components usually dominate unless ϵ_e is very small. Figure 1a displays the broadband spectrum of a long GRB within the internal shock model for a particular choice of parameters [129]. Since the phenomenological shock microphysics is poorly known, modelers usually introduce ϵ_e , ϵ_B , ϵ_p as free parameters. For ϵ_e ’s not too small ($\gtrsim 10^{-3}$), the high energy spectrum is dominated by the electron IC component, as in Fig. 1a. For smaller ϵ_e ’s (e.g. $\epsilon_e = 10^{-3}$), on the other hand, the hadronic components become at least comparable to the leptonic component above ~ 100 GeV, and the π^0 -decay component dominates the spectrum above ~ 10 TeV.

A bright GRB, 080319B, with a plethora of multi-wavelength observations has recently allowed very detailed spectral modelling as a function of time, and it has shown that an additional high energy component may play an important role. For GRB 080319B, the bright optical flash suggests a synchrotron origin for the optical emission and SSC production of the ~ 500 keV gamma-rays [130]. The intensity of these gamma rays would be sufficient to produce a second-order IC peak around 10–100 GeV.

Due to the high photon number density in the emission region of GRBs, high energy photons have an optical depth for photon-photon pair production greater than unity above a critical energy, producing a sharp spectral cutoff, which depends on the unknown bulk Lorentz factor of the fireball and the variability time scale of the central engine, which sets the size of the emission region. Of course, the shape of time-

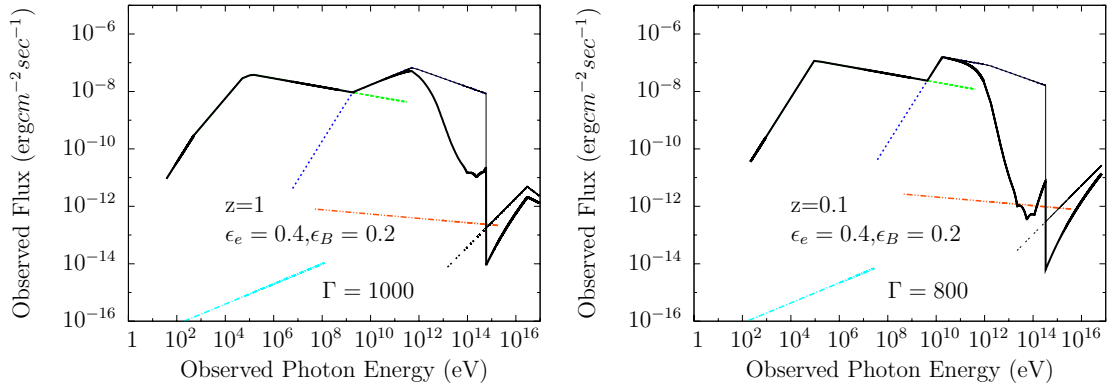


Figure 1: Broad-band spectrum of the GRB prompt emission within the internal shock model (from [129]). (a) A long GRB with the observed sub-MeV luminosity of $\sim 10^{51}$ erg s^{-1} , is modeled for parameters as given in the figure. The solid black lines represent the final spectrum before (thin line) and after (thick line) including the effect of internal optical depths. The long dashed green line (mostly hidden) is the electron synchrotron component; the short-dashed blue line is the electron IC component; the double short-dashed black curve on the right side is the π^0 decay component; the triple short-dashed black line represents the synchrotron radiation produced by e^\pm from π^\pm decays; the dash-dotted (light blue) line represents the proton synchrotron component. (b) The analogous spectrum of a bright short GRB with 10^{51} erg isotropic-equivalent energy release.

integrated spectra will also be modified (probably to power laws rolling over to steeper power laws) due to averaging of evolving instantaneous spectra [131]. For the nominal bulk Lorentz factor $\Gamma = 400$ (as suggested by recent afterglow observations, e.g. [132]) and for a typical variability time scale $t_v = 0.01$ s, the cut off energy is about several tens of GeV. Below 10 GeV, the spectrum is mostly dominated by the electron synchrotron emission, so that with the observed high energy spectrum alone, usually there is no clean differentiation of the leptonic vs. hadronic origin of the high energy gamma-rays. Such an issue may however be addressed by collecting both prompt and afterglow data. Since a small ϵ_e is needed for a hadronic-component-dominated high energy emission, these fireballs must have a very low efficiency for radiation, $\lesssim \epsilon_e$, and most of the energy will be carried by the afterglow. As a result, a moderate-to-high radiative efficiency would suggest a leptonic origin of high energy photons, while a GRB with an extremely low radiative efficiency but an extended high energy emission component would be consistent with (but not a proof for) the hadronic origin. If the fireball has a much larger Lorentz factor ($\gtrsim 800$), the spectral cutoff energy is higher, as in Fig. 1. This would allow a larger spectral space to diag-

nose the origin of the GRB high energy emission and would place the cutoff energies in the spectral region that can only be addressed by VHE telescopes. At even higher energies, the fireball again becomes transparent to gamma rays [77], so that under ideal conditions, the \sim PeV component due to π^0 decay can escape the fireball. Emission above one TeV escaping from GRBs would suffer additional external attenuation by the cosmic infrared background (CIB) and the cosmic microwave background (CMB), thus limiting VHE observations of GRBs to lower redshifts (e.g. $z \lesssim 0.5-1$).

The external shock origin of prompt emission is less favored by the Swift observations, which show a rapidly falling light curve following the prompt emission before the emergence of a more slowly decaying component attributed to the external shock. A small fraction of bursts lack the initial steep component, in which case the prompt emission may result from an external shock. Photons up to TeV energies are expected in the external shock scenario [136], and the internal pair cut-off energy should be very high, more favorable to detection at VHE energies, because of the less compact emission region.

The ‘‘cannonball model’’ of GRBs [133], in which the prompt GRB emission is produced by IC

scattering from blobs of relativistic material (“cannonballs”), can also be used to explain the keV/MeV prompt emission, but it does not predict significant VHE emission during the prompt phase. Sensitive VHE observations would provide a strong constraint to differentiate between these models. The cannonball model could still produce delayed VHE emission during the deceleration phase, in much the same way as the fireball model: as a consequence of IC scattering from relativistic electrons accelerated by the ejecta associated with the burst [134].

1.3.2 Deceleration phase

A GRB fireball would be significantly decelerated by the circumburst medium starting from a distance of $10^{16} - 10^{17}$ cm from the central engine, at which point a pair of shocks propagate into the circumburst medium and the ejecta, respectively. Both shocks contain a similar amount of energy. Electrons from either shock region would Compton scatter the soft seed synchrotron photons from both regions to produce high energy photons [52, 70, 71, 135, 136, 137, 138]. Compared with the internal shock radius, the deceleration radius corresponds to a low “compactness” so that high energy photons more readily escape from the source. Figure 2(a) presents the theoretical forward shock high energy emission components as a function of time for the regime of IC dominance (from [135]). It is evident that during the first several minutes of the deceleration time, the high energy emission could extend to beyond ~ 10 TeV. Detection of this emission by ground-based VHE detectors, for sources close enough to have little absorption by the IR background, would be an important test of this paradigm.

Various IC processes have been considered to interpret the distinct high energy component detected in GRB 941017 [4, 70]. For preferable parameters, the IC emission of forward shock electrons off the self-absorbed reverse shock emission can interpret the observed spectrum (Fig. 2b, [71]).

1.3.3 Steep decay

Swift observations revealed new features of the GRB afterglow. A canonical X-ray lightcurve generally consists of five components [140, 141]: a steep decay component (with decay index ~ -3 or steeper), a shallow decay component (with decay index ~ -0.5 but with a wide variation), a normal decay component (with decay index ~ -1.2), a putative post-jet-break component seen in a small group of GRBs at later times, and multiple X-ray flares with sharp rise and decay occurring in nearly half GRBs. Not all five components appear in every GRB, and the detailed afterglow measurements of GRB 080319B [130] present some challenges to the standard picture we describe here. The steep decay component [142] is generally interpreted as the tail of the prompt gamma-ray emission [140, 141, 143]. Within this interpretation, the steep decay phase corresponds to significant reduction of high energy flux as well. On the other hand, Ref. [14] suggests that the steep decay is the phase when the blastwave undergoes a strong discharge of its hadronic energy. Within such a scenario, strong high energy emission of hadronic origin is expected. Detection/non-detection of strong high energy emission during the X-ray steep decay phase would greatly constrain the origin of the steep decay phase.

1.3.4 Shallow decay

The shallow decay phase following the steep decay phase is still not well understood [144, 145, 146]. The standard interpretation is that the external forward shock is continuously refreshed by late energy injection, either from a long-term central engine, or from slower shells ejected in the prompt phase [140, 141, 147, 148]. Other options include delay of transfer of the fireball energy to the medium [149], a line of sight outside the region of prominent afterglow emission [150], a two-component jet model [151], and time varying shock micro-physics parameters [151, 152, 153].

Since the pre-Swift knowledge of the afterglow

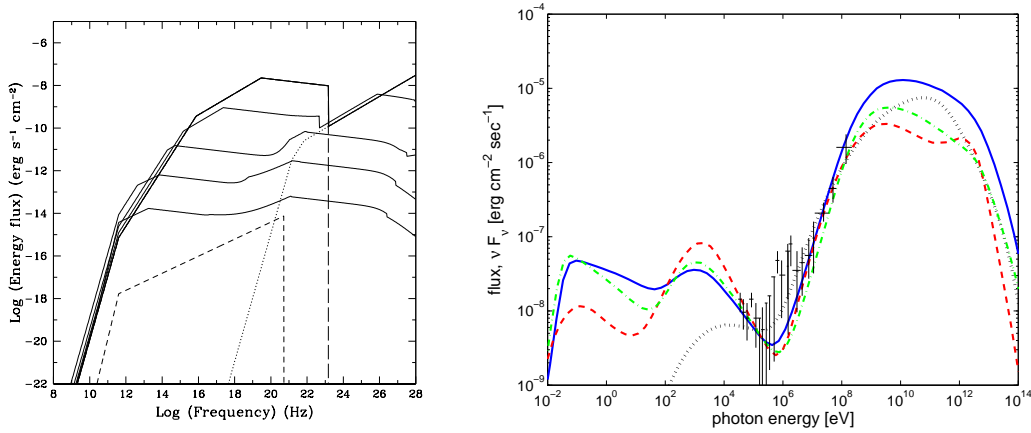


Figure 2: (a) The SSC emission from the forward shock region in the deceleration phase. Temporal evolution of the theoretical models for synchrotron and SSC components for $\epsilon_e = 0.5$, $\epsilon_B = 0.01$; solid curves from top to bottom are at onset, 1 min, 1 hour, 1 day, 1 month. The contributions to the emission at onset are shown as long-dashed (electron-synchrotron), short-dashed (proton-synchrotron) and dotted (electron IC) curves [135]. (b) Fit to the prompt emission data of GRB 941017 using the IC model of Ref. [71].

kinetic energy comes from the late afterglow observations, the existence of the shallow decay phase suggests that the previously estimated external SSC emission strength is over-estimated during the early afterglow. A modified SSC model including the energy injection effect indeed gives less significant SSC flux [154, 155]. The SSC component nonetheless is still detectable by Fermi and higher energy detectors for some choices of parameters. Hence, detections or limits from VHE observations constrain those parameters. If, however, the shallow decay phase is not the result of a smaller energy in the afterglow shock at early times, compared to later times, but instead due to a lower efficiency in producing the X-ray luminosity, the luminosity at higher photon energies could still be high, and perhaps comparable to (or even in excess of) pre-Swift expectations. Furthermore, the different explanations for the flat decay phase predict different high-energy emission, so the latter could help distinguish between the various models. For example, in the energy injection scenario, the reverse shock is highly relativistic for a continuous long-lived relativistic wind from the central source, but only mildly relativistic for an outflow that was ejected during the prompt GRB with a wide range of Lorentz factors and that gradually catches up with the afterglow shock. The dif-

ferent expectations for the high-energy emission in these two cases may be tested against future observations.

1.3.5 High-energy photons associated with X-ray flares

X-ray flares have been detected during the early afterglows in a significant fraction of gamma-ray bursts (e.g. [156, 157, 158]). The amplitude of an X-ray flare with respect to the background afterglow flux can be up to a factor of ~ 500 and the fluence can approximately equal the prompt emission fluence (e.g. GRB 050502B [156, 159]). The rapid rise and decay behavior of some flares suggests that they are caused by internal dissipation of energy due to late central engine activity [140, 156, 159, 160]. There are two likely processes that can produce very high energy (VHE) photons. One process is that the inner flare photons, when passing through the forward shocks, would interact with the shocked electrons and get boosted to higher energies. Another process is the SSC scattering within the X-ray flare region [155, 161].

Figure 3 shows an example of IC scattering of flare photons by the afterglow electrons for a flare of duration δt superimposed upon an underlying power law X-ray afterglow around time

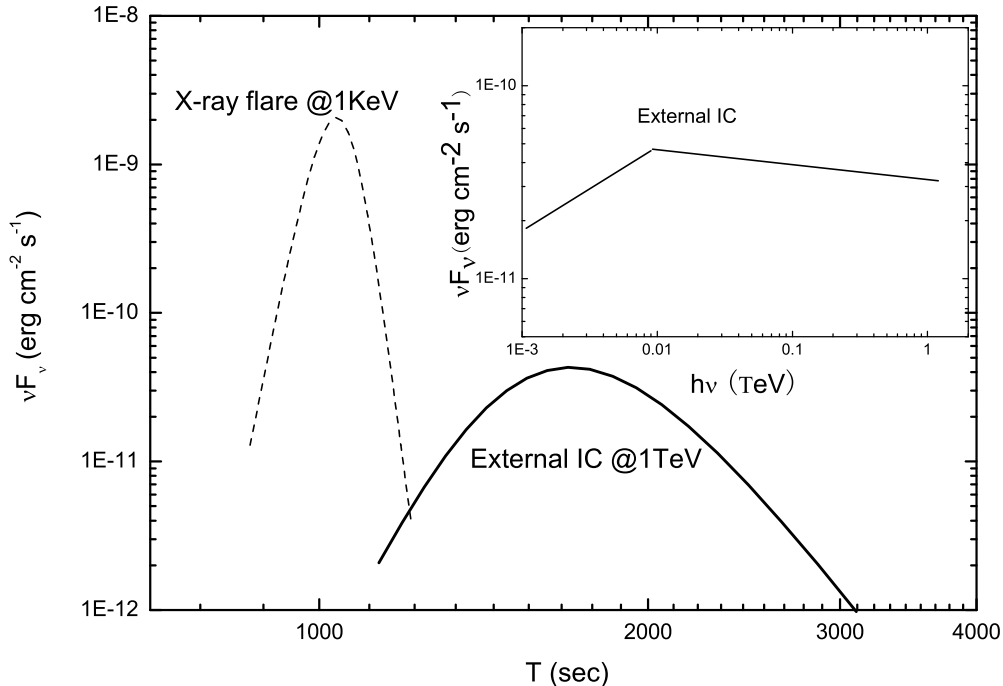


Figure 3: The expected light curves (main figure) and spectral energy distribution (insert figure) of IC scattering of X-ray flare photons by forward shock electrons. The flux is calculated according to [161], based on the following parameters: 10^{53} erg blast wave energy, electron energy distribution index 2.2, electron equipartition factor $\epsilon_e = 0.1$, 1 keV peak energy of the X-ray flare, $10^{28.5}$ cm source distance and that the flare has $\delta t/t_f = 0.3$.

$t_f = 1000$ s after the burst, as observed in GRB 050502B. The duration of the IC emission is lengthened by the angular spreading effect and the anisotropic scattering effect as well [155, 161]. Using the calculation of [161], for typical parameters as given in the caption, νF_ν at 1 TeV reaches about 4×10^{-11} erg cm $^{-2}$ s $^{-1}$, with a total duration of about 2000 s.

The peak energy of the SSC scattering within the X-ray flare region lies at tens of MeV [161] to a few hundreds of MeV [155]. The flares may come from internal dissipation processes similar to the prompt emission, so their dissipation radius may be much smaller than that of the afterglow external shock. A smaller dissipation radius causes strong internal absorption to very high energy photons. For a flare with luminosity $L_x \sim 10^{48}$ erg s $^{-1}$ and duration $\delta t = 100$ s, the VHE photons can escape only if the dissipation radius is larger than $\sim 10^{16}$ cm. So in general, even for a strong X-ray flare occurring at small dissipation radius, the SSC emission at TeV energies should

be lower than the IC component above.

1.3.6 High-energy photons from external reprocessing

Very high energy photons above 100 GeV produced by GRBs at cosmological distances are subject to photon-photon attenuation by the CIB (e.g. [162, 163]) and CMB. The attenuation of E TeV photons by the CIB would produce secondary electron-positron pairs with a Lorentz factor of $\gamma_e \simeq 10^6 E$, which in turn IC scatter off CMB photons to produce MeV–GeV emission [77, 164, 165, 166]. This emission is delayed relative to the primary photons by two mechanisms: one is the opening angles of the scattering processes, producing a deviation from the direction of the original TeV photons by an angle $1/\gamma_e$; the other is the deflection of the secondary pairs in the intergalactic magnetic field [167]. Only if the intergalactic magnetic field is less than $\sim 10^{-16}$ G would the delayed secondary gamma-rays still be beamed from the same direction as the GRB.

1.4 High Energy Emission Predictions for Short Bursts

Recent observational breakthroughs [168, 169, 170, 171, 172] suggest that at least some short GRBs are nearby low-luminosity GRBs that are associated with old stellar populations and likely to be compact star mergers. The X-ray afterglows of short duration GRBs are typically much fainter than those of long GRBs, which is consistent with having a smaller total energy budget and a lower density environment as expected from the compact star merger scenarios. Observations suggest that except being fainter, the afterglows of short GRBs are not distinctly different from those of long GRBs. The long duration GRB 060614 has a short, hard emission episode followed by extended softer emission. It is a nearby GRB, but has no supernova association, suggesting that 060614-like GRBs are more energetic versions of short GRBs [173, 174].

The radiation physics of short GRBs is believed to be similar to that of long GRBs. As a result, all the processes discussed above for long GRBs are relevant to short GRBs as well. The predicted prompt emission spectrum of a bright short GRB is presented in Fig. 1b [129]. Figure 1b is calculated for a comparatively bright, 1-second burst at redshift 0.1 with isotropic-equivalent luminosity 10^{51} erg s⁻¹. Fig. 1b suggests that the high energy component of such a burst is barely detectable by Fermi. Due to internal optical depth, the spectrum is cut off beyond about 100 GeV. VHE observations can constrain the bulk Lorentz factor, since VHE emission can be achievable if the bulk Lorentz factor is even larger (e.g. 1000 or above).

No evidence of strong reverse shock emission from short GRBs exists. For the forward shock, the flux is typically nearly 100 times fainter than that of long GRBs. This is a combination of low isotropic energy and presumably a low ambient density. The SSC component in the forward shock region still leads to GeV-TeV emission, but the flux is scaled down by the same factor as the low energy afterglows. Multiple late-time X-ray flares have been detected for some short

GRBs (e.g. GRB 070724 and GRB 050724), with at least some properties similar to the flares in long GRBs, so that the emission mechanisms discussed above for long GRB flares may also apply, scaled down accordingly. In general, short GRBs may be less prominent emitters of high energy photons than long GRBs, mainly due to their low fluence observed in both prompt emission and afterglows. A potential higher bulk Lorentz factor on the other hand facilitates the escaping of 100 GeV or even TeV photons from the internal emission region. Furthermore, a few short GRBs are detected at redshifts lower than 0.3, and the average short GRB redshift is much lower than that of long GRBs. This is favorable for TeV detection since the CIB absorption is greatly reduced at these redshifts.

1.5 Supernova-associated gamma-ray bursts

Nearby GRBs have been associated with spectroscopically identified supernovae, *e.g.*, GRB 980425/SN 1998bw, GRB 031203/SN 2003lw, GRB 060218/SN 1006aj, and GRB 030329/SN 2003lw. The processes discussed in the section on high-energy emission from long GRBs can all apply in these bursts, and with their close distances, VHE emission from these sources would not be significantly attenuated by the CIB. These bursts have low luminosity, but the internal absorption by soft prompt emission photons may therefore be lower, so that VHE photons originating from the internal shock are more likely to escape without significant absorption, compensating for the overall low flux. In addition, if there is a highly relativistic jet component associated with the supernovae, supernova shock breakout photons would be scattered to high energies by the shock-accelerated electrons in the forward shocks [175]. The strong thermal X-ray emission from GRB 060218 may be such a relativistic supernova shock breakout [128, 176]. It has been shown [175] that if the wind mass loss rate from the progenitor star is low, the $\gamma\gamma$ absorption cutoff energy at early times can be larger than ~ 100 GeV, so VHE emission could

be detected from these nearby SN-GRBs.

1.6 Ultra High Energy Cosmic Rays and GRBs

The origin of the UHE cosmic rays (UHECR) is an important unsolved problem. The idea that they originate from long duration GRBs is argued for a number of reasons. First, the power required for the cosmic rays above the “ankle” ($\sim 10^{19}$ eV) is within one or two orders of magnitude equal to the hard X-ray/ γ -ray power of BATSE GRBs, assumed to be at average redshift unity [177, 178, 179]. Second, GRBs form powerful relativistic flows, providing extreme sites for particle acceleration consistent with the known physical limitations, e.g. size, required to achieve ultra high energy. Third, GRBs are expected to be associated with star-forming galaxies, so numerous UHECR sources would be found within the ~ 100 Mpc GZK radius, thus avoiding the situation that there is no persistent powerful source within this radius. And, finally, various features in the medium- and high-energy γ -ray spectra of GRBs may be attributed to hadronic emission processes.

The required Lorentz factors of UHECRs, $\gtrsim 10^{10}$, exceed by orders of magnitude the baryon-loading parameter $\eta \gtrsim 100$ thought typical of GRB outflows. Thus the UHECRs must be accelerated by processes in the relativistic flows. The best-studied mechanism is Fermi acceleration at shocks, including external shocks when the GRB blast wave interacts with the surrounding medium, and internal shocks formed in an intermittent relativistic wind.

Protons and ions with nuclear charge Z are expected to be accelerated at shocks, just like electrons. The maximum energy in the internal shock model [177] or in the case of an external shock in a uniform density medium [180, 181] are both of order a few $Z 10^{20}$ eV for typical expected burst parameters. Thus GRBs can accelerate UHECRs. The ultrarelativistic protons/ions in the GRB jet and blast wave can interact with ambient soft photons if the corresponding opacity is of the order of unity or

higher, to form escaping neutral radiations (neutrons, γ -rays, and neutrinos). They may also interact with other baryons via inelastic nuclear production processes, again producing neutrals. So VHE gamma rays are a natural consequence of UHECR acceleration in GRBs. While leptonic models explain keV–MeV data as synchrotron or Compton radiation from accelerated primary electrons, and GeV–TeV emission from inverse-Compton scattering, a hadronic emission component at GeV–TeV energies can also be present.

Neutrons are coupled to the jet protons by elastic p - n nuclear scattering and, depending on injection conditions in the GRB, can decouple from the protons during the expansion phase. As a result, the neutrons and protons travel with different speeds and will undergo inelastic p - n collisions, leading to π -decay radiation, resulting in tens of GeV photons [93, 94]. The decoupling leads to subsequent interactions of the proton and neutron-decay shells, which may reduce the shell Lorentz factor by heating [95]. The n - p decoupling occurs in short GRBs for values of the baryon-loading parameter $\eta \sim 300$ [182]. The relative Lorentz factor between the proton and neutron components may be larger than in long duration GRBs, leading to energetic (~ 50 GeV) photon emission. Applying this model to several short GRBs in the field of view of Milagro [183] gives fluxes of a few 10^{-7} cm $^{-2}$ s $^{-1}$ for typical bursts, suggesting that a detector of large effective area, $\gtrsim 10^7$ cm 2 , at low threshold energy is needed to detect these photons. For the possibly nearby ($z = 0.001$) GRB 051103, the flux could be as large as $\sim 10^{-3}$ cm $^{-2}$ s $^{-1}$.

Nuclei accelerated in the GRB jet and blast wave to ultra high energies can make γ -rays through the synchrotron process; photopair production, which converts the target photon into an electron-positron pair with about the same Lorentz factor as the ultrarelativistic nucleus; and photopion production, which makes pions that decay into electrons and positrons, photons, and neutrinos. The target photons for the latter two processes are usually considered to be the ambient synchrotron and synchrotron self-Compton photons formed by leptons accelerated

at the forward and reverse shocks of internal and external shocks. If the pion-decay muons decay before radiating much energy [184], the secondary leptons, γ -rays, and neutrinos each carry about 5% of the primary energy.

About one-half of the time, neutrons are formed in a photopion reaction. If the neutron does not undergo another photopion reaction before escaping the blast wave, it becomes free to travel until it decays. Neutrons in the neutral beam [185], collimated by the bulk relativistic motion of the GRB blast wave shell, travel $\approx (E_n/10^{20} \text{ eV}) \text{ Mpc}$ before decaying. A neutron decays into neutrinos and electrons with $\approx 0.1\%$ of the energy of the primary. Ultrarelativistic neutrons can also form secondary pions after interacting with other soft photons in the GRB environment. The resulting decay electrons form a hyper-relativistic synchrotron spectrum, which is proposed as the explanation for the anomalous γ -ray emission signatures seen in GRB 941017 [186].

The electromagnetic secondaries generate an electromagnetic cascade when the optical depth is sufficiently large. The photon number index of the escaping γ -rays formed by multiple generations of Compton and synchrotron radiation is generally between $-3/2$ and -2 below an exponential cutoff energy, which could reach to GeV or, depending on parameter choices, TeV energies [87, 185].

Gamma-ray observations of GRBs will help distinguish between leptonic and hadronic emissions. VHE γ -ray emission from GRBs can be modeled by synchro-Compton processes of shock-accelerated electrons [33, 53, 54, 58, 136], or by photohadronic interactions of UHECRs and subsequent cascade emission [83, 187, 188], or by a combined leptonic/hadronic model. The clear distinction between the two models from γ -ray observation will not be easy. The fact that the VHE γ -rays are attenuated both at their production sites and in the CIB restricts measurements to energies below 150 GeV ($z \sim 1$) or 5 TeV ($z \lesssim 0.2$). Distinctive features of hadronic models are:

- Photohadronic interactions and subsequent electromagnetic γ -ray producing cascades develop over a long time scale due to slower energy loss-rate by protons than electrons. The GeV-TeV light curves arising from hadronic mechanisms then would be longer than those expected from purely leptonic processes [83], facilitating detection with pointed instruments.
- Cascade γ rays will be harder than a -2 spectrum below an exponential cutoff energy, and photohadronic processes can make hard, ~ -1 spectra from anisotropic photohadronic-induced cascades, used to explain GRB 941017 [4, 186]. A “two zone” leptonic synchro-Compton mechanism can, however, also explain the same observations [70, 71, 135, 189], with low energy emission from the prompt phase and high energy emission from a very early afterglow.
- Another temporal signature of hadronic models is delayed emission from UHECR cascades in the CIB/CMB [190] or $\gtrsim \text{PeV}$ energy γ -rays, from π^0 decay, which may escape the GRB fireball [77]. However, $\gtrsim \text{TeV}$ photons created by leptonic synchro-Compton mechanism in external forward shocks may imitate the same time delay by cascading in the background fields [166].
- Quasi-monoenergetic π^0 decay γ -rays from n - p decoupling, which are emitted from the jet photosphere prior to the GRB, is a promising hadronic signature [93, 94, 182], though it requires that the GRB jet should contain abundant free neutrons as well as a large baryon load.

Detection of high-energy neutrino emissions would conclusively demonstrate cosmic ray acceleration in GRBs, but non-detection would not conclusively rule out GRBs as a source of UHECRs, since the ν production level even for optimistic parameters is small.

1.7 Tests of Lorentz Invariance with Bursts

Due to quantum gravity effects, it is possible that the speed of light is energy dependent and that $\Delta c/c$ scales either linearly or quadratically with $\Delta E/E_{QG}$, where E_{QG} could be assumed to be at or below the Planck energy, E_P [191, 192, 193]. Recent detections of flaring from the blazar Mrk 501, using the MAGIC IACT, have used this effect to constrain the quantum gravity scale for linear variations to $\gtrsim 0.1E_P$ [194]. This same technique could be applied to GRBs, which have fast variability, if they were detected in the TeV range and if the intrinsic chromatic variations were known. However, there may be intrinsic limitations to some approaches [195]. By improving the sensitivity and the energy range with a future telescope array, the current limit could be more tightly constrained, particularly if it were combined with an instrument such as Fermi at lower energies, thus increasing the energy lever arm.

1.8 Detection Strategies for VHE Gamma-Ray Burst Emission

Ground-based observations of TeV emission from gamma ray bursts are difficult. The fraction of GRBs close enough to elude attenuation at TeV energies by the CIB is small. Only $\sim 10\%$ of long bursts are within $z < 0.5$, the redshift of the most distant detected VHE source, 3C 279 [121]. Short bursts are more nearby with over 50% detected within $z < 0.5$, but the prompt emission has ended prior to satellite notifications of the burst location.

Therefore, wide field of view detectors with high duty cycle operations would be ideal to observe the prompt emission from gamma-ray bursts. Imaging atmospheric Cherenkov telescopes (IACT) can be made to cover large sections of the sky by either having many mirrors each pointing in a separate direction or by employing secondary optics to expand the field of view of each mirror. However, the duty factor is still $\sim 10\%$ due to solar, lunar, and weather

constraints. IACTs could also be made with fast slewing mounts to allow them to slew to most GRBs within ~ 20 seconds, thus allowing them to observe some GRBs before the end of the prompt phase. Alternatively, extensive air shower detectors intrinsically have a field of view of ~ 2 sr and operate with $\sim 95\%$ duty factor. These observatories, especially if located at very high altitudes, can detect gamma rays down to 100 GeV, but at these low energies they lack good energy resolution and have a point spread function of ~ 1 degree. The traditionally less sensitive extensive air shower detectors may have difficulty achieving the required prompt emission sensitivity on short timescales ($> 5\sigma$ detection of 10^{-9} erg s^{-1} cm^{-2} in $\lesssim 20$ sec integration). The combined observations of both of these types of detectors would yield the most complete picture of the prompt high energy emission. The expected performance of the two techniques relative to a particular prompt GRB emission model is shown in Figure 4.

The detector strategy for extended emission associated with traditional afterglows or with late-time flares from GRBs is far simpler than the strategy for early prompt emission. The high sensitivity and low energy threshold of an IACT array are the best way to capture photons from this emission at times greater than ~ 1 min, particularly if fast slewing is included in the design.

1.9 Synergy with other instruments

While GRB triggers are possible from wide angle VHE instruments, a space-based GRB detector will be needed. Swift, Fermi, or future wide field of view X-ray monitors such as EXIST or JANUS must provide lower energy observations. GRBs with observations by both Fermi and VHE telescopes will be particularly exciting and may probe high Lorentz factors. Neutrino telescopes such as IceCube, UHECR telescopes such as Auger, and next generation VHE observatories can supplement one another in the search for UHECRs from GRBs, since neutrinos are expected along with VHE gamma rays. Detection of gravitational waves from GRB pro-

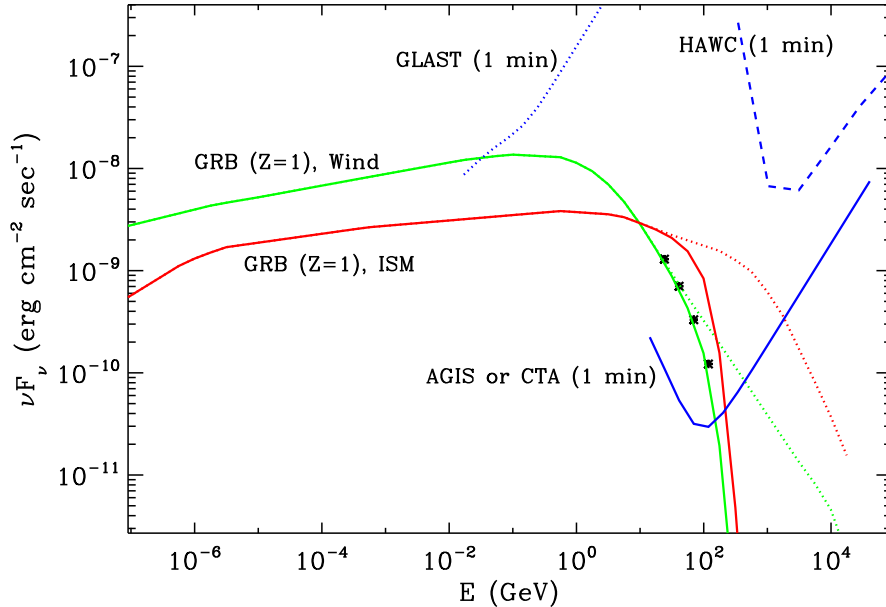


Figure 4: A plot of the predicted gamma-ray spectrum from a GRB at a redshift of $z=1$ adapted from Pe’er and Waxman [196], reduced by a factor of 10 to illustrate the sensitivity even to weaker bursts. The green and red curves show the calculation for a wind environment and an ISM-like environment. The dotted curves give the source spectrum, while the solid curves include the effects of intergalactic absorption using a model from Franceschini et al. [197]. The blue curves show the differential sensitivity curves for Fermi (GLAST; dotted), a km^2 IACT array like AGIS or CTA (solid) and the HAWC air shower array (dashed). For the AGIS/CTA curve we show the differential sensitivity for 0.25 decade bins, while for the HAWC instrument we assume 0.5 decade bins. The sensitivity curve is based on a 5 sigma detection and at least 25 detected photons. Black points and error bars (not visible) are simulated independent spectral points that could be obtained with AGIS/CTA.

genitors with instruments such as LIGO have the potential to reveal the engine powering the GRB fireball. Correlated observations between gravitational wave observatories and VHE gamma-ray instruments will then be important for understanding which type(s) of engine can power VHE emission.

Correlated observations between TeV gamma-ray detectors and neutrino detectors have the potential for significant reduction in background for the participants. If TeV gamma sources are observed, observers will know where and when to look for neutrinos (and vice versa [198], though the advantage in that direction is less significant). For example, searches for GRB neutrinos have used the known time and location to reduce the background by a factor of nearly 10^5 compared to an annual all-sky diffuse search [199]. Beyond decreasing background, correlated ob-

servations also have the potential to increase the expected signal rate. If the spectrum of high-energy gamma rays is known, then constraints on the expected neutrino spectrum can also be introduced, allowing the signal-to-noise ratio of neutrino searches to be significantly improved [200]. In the case of the AMANDA GRB neutrino search, which is based on a specific theoretical neutrino spectrum, the expected signal collection efficiency is nearly 20 times higher than the less constrained search for diffuse UHE neutrinos. With combined photon and neutrino observational efforts, there is a much better chance of eventual neutrino detection of sources such as GRBs (and AGN).

1.10 Conclusions

Gamma-ray bursts undoubtedly involve a population of high-energy particles responsible for the emission detected from all bursts (by definition) at energies up to of order 1 MeV, and for a few bursts so far observable by EGRET, up to a few GeV. Gamma-ray bursts may in fact be the source of the highest energy particles in the universe. In virtually all models, this high-energy population can also produce VHE gamma-rays, although in many cases the burst environment would be optically thick to their escape. The search for and study of VHE emission from GRB therefore tests theories about the nature of these high energy particles (Are they electrons or protons? What is their spectrum?) and their environment (What are the density and bulk Lorentz factors of the material? What are the radiation fields? What is the distance of the emission site from the central source?). In addition, sensitive VHE measurements would aid in assessing the the total calorimetric radiation output from bursts. Knowledge of the VHE gamma-ray properties of bursts will therefore help complete the picture of these most powerful known accelerators.

An example of the insight that can be gleaned from VHE data is that leptonic synchrotron/SSC models can be tested, and model parameters extracted, by correlating the peak energy of X-ray/soft γ -ray emission with GeV–TeV data. For long lived GRBs, the spectral properties of late-time flaring in the X-ray band can be compared to the measurements in the VHE band, where associated emission is expected. Of clear interest is whether there are distinctly evolving high-energy γ -ray spectral components, whether at MeV, GeV or TeV energies, unaccompanied by the associated lower-energy component expected in leptonic synchro-Compton models. Emission of this sort is most easily explained in models involving proton acceleration. As a final example, the escape of VHE photons from the burst fireball provides a tracer of the minimum Doppler boost and bulk Lorentz motion of the emission region along the line of site, since the inferred

opacity of the emission region declines with increasing boost.

There are observational challenges for detecting VHE emission during the initial prompt phase of the burst. The short duration of emission leaves little time (tens of seconds) for repointing an instrument, and the opacity of the compact fireball is at its highest. For the majority of bursts having redshift $\gtrsim 0.5$, the absorption of gamma rays during all phases of the burst by collisions with the extragalactic background light reduces the detectable emission, more severely with increasing gamma-ray energy. With sufficient sensitivity, an all-sky instrument is the most desirable for studying the prompt phase, in order to measure the largest sample of bursts and to catch them at the earliest times. As discussed in the report of the Technology Working Group, the techniques used to implement all-sky compared to pointed VHE instruments result in a trade-off of energy threshold and instantaneous sensitivity for field of view. More than an order of magnitude improvement in sensitivity to GRBs is envisioned for the next-generation instruments of both types, giving both approaches a role in future studies of GRB prompt emission.

The detection of VHE afterglow emission, delayed prompt emission from large radii, and/or late X-ray flare-associated emission simply requires a sensitive instrument with only moderate slew speed. It is likely that an instrument with significant sensitivity improvements over the current generation of IACTs will detect GRB-related VHE emission from one or all of these mechanisms which do not suffer from high internal absorption, thus making great strides towards understanding the extreme nature and environments of GRBs and their ability to accelerate particles.

In conclusion, large steps in understanding GRBs have frequently resulted from particular new characteristics measured for the first time in a single burst. New instruments improving sensitivity to very-high-energy gamma-rays by an order or magnitude or more compared to existing observations have the promise to make just such a breakthrough in the VHE band.

References

- [1] K. Hurley et al., 1994, *Nature* 372, 652
- [2] B. L. Dingus, 1995, *Astrophys. Space Sci.* 231, 187
- [3] B. L. Dingus, J. R. Catelli, & E. J. Schneid, 1998, *AIP Conf. Proc.* 428, 349
- [4] M. M. González et al., 2003, *Nature* 424, 749
- [5] R. Atkins et al., 2000, *Astrophys. J. Lett.* 533, L119
- [6] R. Atkins et al., 2003, *Astrophys. J.* 583, 824
- [7] Paczyński, B. 1986, *Astrophys. J.*, 308, L43
- [8] Goodman, J. 1986, *Astrophys. J.*, 308, L43
- [9] Paczyński, B. 1990, *Astrophys. J.*, 363, 218
- [10] Paczyński, B., & Xu, G. 1994, *Astrophys. J.*, 427, 708
- [11] Rees, M.J., & Mészáros, P. 1994, *Astrophys. J.*, 430, L93
- [12] Rees, M.J., & Mészáros, P. 1992, *Mon. Not. Roy. Astron. Soc.*, 258, 41
- [13] Dermer, C.D., & Mitman, K.E. 1999, *Astrophys. J.*, 513, L5
- [14] Dermer, C. 2007, *Astrophys. J.*, 664, 384
- [15] Kazimura, Y., et al. 1998, *Astrophys. J.*, 498, L183
- [16] Silva, L.O., et al. 2003, *Astrophys. J.*, 596, L121
- [17] Frederiksen, J.T., et al. 2004, *Astrophys. J.*, 608, L13
- [18] Nishikawa, K.-I., et al. 2005, *Astrophys. J.*, 622, 927
- [19] Spitkovsky, A. 2008, arXiv:0802.3216
- [20] Panaitescu, A., & Mészáros, P. 1998, *Astrophys. J.*, 492, 683
- [21] Thompson, C. 1994, *Mon. Not. Roy. Astron. Soc.*, 270, 480
- [22] Usov, V. V. 1992, *Nature*, 357, 472
- [23] Mészáros, P., & Rees, M.J. 1997, *Astrophys. J.*, 482, L29
- [24] Drenkhahn, G. 2002, *A&A*, 387, 714
- [25] Drenkhahn, G., & Spruit, H. 2002, *A&A*, 391, 1141
- [26] Lyutikov, M., & Blandford, R. 2003, *astro-ph/0312347*
- [27] Giannios, D., & Spruit, H. 2005, *A&A*, 430, 1
- [28] Kumar, P. 1999, *Astrophys. J.*, 523, L113
- [29] Panaitescu, A., Spada, M., & Mészáros, P. 1999, *Astrophys. J.*, 522, L105
- [30] Mészáros, P., Laguna, P., & Rees, M.J. 1993, *Astrophys. J.*, 415, 181
- [31] Mészáros, P., & Rees, M.J. 1993, *Astrophys. J.*, 418, L59
- [32] Katz, J.I. 1994, *Astrophys. J.*, 432, L107
- [33] Pe'er, A., & Waxman, E. 2004, *Astrophys. J.*, 613, 448
- [34] Tavani, M. 1996, *Astrophys. J.*, 466, 768
- [35] Tavani, M. 1996, *Phys. Rev. Lett.*, 76, 3478
- [36] Cohen, E., et al. 1997, *Astrophys. J.*, 488, 330
- [37] Crider, A., et al. 1997, *Astrophys. J.*, 479, L39
- [38] Preece, R.D., et al. 1998, *Astrophys. J.*, 506, L23
- [39] Frontera, F., et al. 2000, *Astrophys. J.*, 527, 59
- [40] Preece, R.D., et al. 2002, *Astrophys. J.*, 581, 1248
- [41] Ghirlanda, G., Celotti, A., & Ghisellini, G. 2003, *A&A*, 406, 879
- [42] Medvedev, M.V. 2000, *Astrophys. J.*, 540, 704
- [43] Lloyd, N.M., & Petrosian, V. 2000, *Astrophys. J.* 543, 722
- [44] Lloyd-Ronning, N.M., & Petrosian, V. 2002, *Astrophys. J.*, 565, 182
- [45] Dermer, C.D., & Böttcher, M. 2000, *Astrophys. J.*, 534, L155
- [46] Granot, J., Piran, T., Sari 2000, *Astrophys. J.*, 534, L163
- [47] Mészáros, P., & Rees, M.J. 2000, *Astrophys. J.*, 530, 292
- [48] Daigne, F., & Mochkovitch, R. 2002, *Mon. Not. Roy. Astron. Soc.*, 336, 1271

- [49] Mészáros, P., Ramirez-Ruiz, E., Rees, M.J., & Zhang, B. 2002, *Astrophys. J.*, 578, 812
- [50] Ryde, F. 2004, *Astrophys. J.*, 614, 827
- [51] Ryde, F. 2005, *Astrophys. J.*, 625, L95
- [52] Mészáros, P., & Rees, M.J. 1994, *Mon. Not. Roy. Astron. Soc.*, 269, L41
- [53] Mészáros, P., Rees, M.J., & Papathanassiou, H. 1994, *Astrophys. J.*, 432, 181
- [54] Papathanassiou, H., & Mészáros, P. 1996, *Astrophys. J.*, 471, L91
- [55] Liang, E. P., Kusunose, M., Smith, I., & Crider, A. 1997, *Astrophys. J.*, 479, L35
- [56] Sari, R., & Piran, T. 1997, *Mon. Not. Roy. Astron. Soc.*, 287, 110
- [57] Pilla, R.P., & Loeb, A. 1998, *Astrophys. J.*, 494, L167
- [58] Chiang, J., & Dermer, C.D. 1999, *Astrophys. J.*, 512, 699
- [59] Panaitescu, A., & Mészáros, P. 2000, *Astrophys. J.*, 544, L17
- [60] Baring, M. & Braby, M. 2004, *Astrophys. J.*, 613, 460
- [61] Rees, M.J., & Mészáros, P. 2005, *Astrophys. J.*, 628, 847
- [62] Pe'er, A., Mészáros, P., & Rees, M.J. 2006, *Astrophys. J.*, 642, 995
- [63] Shaviv, N.J., & Dar, A. 1995, *Astrophys. J.*, 447, 863
- [64] Lazzati, D., Ghisellini, G., Celotti, A., & Rees, M.J. 2000, *Astrophys. J.*, 529, L17
- [65] Broderick, A.E. 2005, *Mon. Not. Roy. Astron. Soc.*, 361, 955
- [66] Inoue, S., Guetta, D., & Pacini, F. 2003, *Astrophys. J.*, 583, 379
- [67] Liang, E. P. 1997, *Astrophys. J.*, 491, L15
- [68] Ghisellini, G., & Celotti, A. 1999, *Astrophys. J.*, 511, L93
- [69] Guetta, D., & Granot, J. 2003, *Astrophys. J.*, 585, 885
- [70] Granot, J., & Guetta, D. 2003, *Astrophys. J.*, 598, L11
- [71] Pe'er, A., & Waxman, E. 2004, *Astrophys. J.*, 603, L1
- [72] Krolik, J. H., & Pier, E.A. 1991, *Astrophys. J.*, 373, 277
- [73] Fenimore, E.E., Epstein, R.I., & Ho, C. 1993, *A&A*, 97, 59
- [74] Woods, E., & Loeb, A. 1995, *Astrophys. J.*, 453, 583
- [75] Baring, M.G., & Harding, A.K. 1997, *Astrophys. J.*, 491, 663
- [76] Lithwick, Y., & Sari, R. 2001, *Astrophys. J.*, 555, 540
- [77] Razzaque, S., Mészáros, P., & Zhang, B. 2004, *Astrophys. J.*, 613, 1072
- [78] Kobayashi, S., & Zhang, B. 2003, *Astrophys. J.*, 597, 455
- [79] Zhang, B., Kobayashi, S. & Mészáros, P. 2003, *Astrophys. J.*, 595, 950
- [80] Pe'er, A. et al. 2007, *Astrophys. J.*, 664, L1
- [81] Gupta, N., Zhang, B., 2008, *Mon. Not. Roy. Astron. Soc.*, 384, L11
- [82] Vietri, M. 1997, *Phys. Rev. Lett.*, 78, 4328
- [83] Böttcher, M., & Dermer, C.D. 1998, *Astrophys. J.*, 499, L131
- [84] Totani, T. 1998, *Astrophys. J.*, 509, L81
- [85] Waxman, E., & Bahcall, J. 1997, *Phys. Rev. Lett.*, 78, 2292
- [86] Waxman, E., & Bahcall, J. 2000, *Astrophys. J.*, 541, 707
- [87] Dermer, C.D., & Atoyan, A. 2003, *Phys. Rev. Lett.*, 91, 071102
- [88] Guetta, D., & Granot, J. 2003, *Phys. Rev. Lett.*, 90, 1103
- [89] Granot, J., & Guetta, D. 2003, *Phys. Rev. Lett.*, 90, 1119
- [90] Dermer, C.D., Ramirez-Ruiz, E. & Le, T. 2007, *Astrophys. J.*, 664, L67
- [91] Katz, J.I. 1994, *Astrophys. J.*, 432, L27
- [92] De Paolis, F., Inghrosso, G., & Orlando, D. 2000, *A&A*, 359, 514
- [93] Derishev, E.V., Kocharovskiy, V.V., & Kocharovskiy, V.I. 2001, *Astrophys. J.*, 521, 640
- [94] Bahcall, J.N., & Mészáros, P. 2000, *Phys. Rev. Lett.*, 85, 1362

- [95] Rossi, E., Beloborodov, A.M., & Rees, M.J. 2006, *Mon. Not. Roy. Astron. Soc.*, 369, 1797
- [96] Rees, M.J., & Mészáros, P. 1998, *Astrophys. J.*, 496, L1
- [97] Granot, J., Nakar, E., & Piran, T. 2003, *Nature*, 426, 138
- [98] Kumar, P., & Piran, T. 2000, *Astrophys. J.*, 535, 152
- [99] Wang, X., & Loeb, A. 2000, *Astrophys. J.*, 535, 788
- [100] Nakar, E., Piran, T., & Granot, J. 2003, *NewA*, 8, 495
- [101] Wijers, R.A.M.J. 2001, in *Gamma Ray Bursts in the Afterglow Era*, ed. E. Costa, Frontera. F. and Hjorth J. (Springer: Berlin) 306
- [102] Ramirez-Ruiz, E., García-Segura, G., Salmonson, J.D., & Pérez-Rendón, B. 2005, *Astrophys. J.*, 631, 435
- [103] Pe'er, A., & Wijers, R.A.M.J. 2006, *Astrophys. J.*, 643, 1036
- [104] Nakar, E. & Granot, J. 2007, *Mon. Not. Roy. Astron. Soc.*, 380, 1744
- [105] Genet, F., Daigne, F., & Mochkovitch, R. 2007, *Mon. Not. Roy. Astron. Soc.*, 381, 732
- [106] Uhm, Z., & Beloborodov, A. 2007, *Astrophys. J.*, 665, 93
- [107] Padilla, L., et al. 1998, *A&A*, 337, 43
- [108] Amenomori, M., et al. 2001, *AIP Conf. Proc.*, 558, 844
- [109] Atkins, R., et al. 2005, *ApJ*, 630, 996
- [110] Saz Parkinson, P. M. 2007, *AIP Conf. Proc.* 921, 470
- [111] Abdo, A. A., et al. 2007, *ApJ*, 666, 361
- [112] Atkins, R., et al. 2004, *ApJ*, 604, L25
- [113] Meegan, C. A., et al. 1992, *Nature*, 355, 143
- [114] Connaughton, V., et al. 1997, *ApJ*, 479, 859
- [115] Horan, D., et al. 2007, *ApJ*, 655, 396
- [116] Albert, J., et al. 2006, *ApJ*, 641, L9
- [117] Bastierei, D., et al. 2007, *Proc. 30th ICRC Merida, Mexico*, ArXiv e-prints 0709.1380
- [118] Albert, J., et al. 2007, *Astrophys. J.* 667, 358
- [119] Bastierei, D., et al. 2007b, *Proc. 30th ICRC Merida, Mexico*, ArXiv e-prints 0709.1386
- [120] Horan, D., et al. 2007b, Paper 406, *Proc. 30th ICRC, Merida, MX*
- [121] Albert, J., et al. 2008, *Science*, 27, 1752
- [122] Woosley, S. E. 1993, *Astrophys. J.*, 405, 273
- [123] MacFadyen, A. I. & Woosley, S. E. 1999, *Astrophys. J.*, 524, 262
- [124] Bloom, J. S. et al. 1999, *Nature*, 401, 453
- [125] Haislip, J. B. et al. 2006, *Nature*, 440, 181
- [126] Berger, E. et al. 2005, *Astrophys. J.*, 634, 501
- [127] Jakobssen, P., Levan, A., Fynbo, J.P.U., et al. 2006, *Astron. & Astrophys.*, 447, 897
- [128] Campana, S. et al. 2006, *Nature*, 442, 1008
- [129] Gupta, N., Zhang, B., 2007, *Mon. Not. Roy. Astron. Soc.*, 380, 78
- [130] Racusin, J. L. et al. 2008, *Nature*, 455, 183
- [131] Granot, J., Cohen-Tanugi, J., do Couto e Silva, E. 2008, *Astrophys. J.*, 677, 92
- [132] Molinari, E. et al. 2007, *A&A*, 469, 13
- [133] Dar, A., & de Rújula, A. 2004, *Phys. Rep.*, 405, 203
- [134] Dado, S., & Dar, A. 2005, *Astrophys. J. Lett.*, 627, L109
- [135] Zhang, B., Mészáros P. 2001, *Astrophys. J.*, 559, 110
- [136] Dermer, C.D., Chiang, J., & Mitman, K.E. 2000, *Astrophys. J.*, 537, 785
- [137] Wang, X. Y., Dai, Z. G., Lu, T. 2001, *Astrophys. J.*, 546, L33
- [138] Wang, X. Y., Dai, Z. G., Lu, T. 2001, *Astrophys. J.*, 556, 1010
- [139] Roming, P. et al. 2006, *Astrophys. J.*, 652, 1416
- [140] Zhang, B. et al., 2006, *Astrophys. J.*, 642, 354
- [141] Nousek, J. A. et al. 2006, *Astrophys. J.*, 642, 389

- [142] Tagliaferri, G. et al. 2005, *Nature*, 436, 985
- [143] Kumar, P. & Panaitescu, A. 2000, *Astrophys. J.*, 541, L51
- [144] Mészáros, P. 2006, *Rev. Prog. Phys.*, 2006, 69, 2259
- [145] Granot, J. 2006, *Il Nuovo Cimento B*, 121, 1073
- [146] Zhang, B. 2007, *ChJAA*, 7, 1
- [147] Panaitescu, A. et al. 2006, *Mon. Not. Roy. Astron. Soc.*, 366, 1357
- [148] Granot, J. & Kumar, P. 2006, *Mon. Not. Roy. Astron. Soc.*, 366, L13
- [149] Kobayashi, S. & Zhang, B. 2007, *Astrophys. J.*, 655, 973
- [150] Eichler, D. & Granot, 2006, *Astrophys. J.*, 641, L5
- [151] Granot, J., Königl, A. & Piran, T. 2006, *Mon. Not. Roy. Astron. Soc.*, 370, 1946
- [152] Ioka, K., Toma, K., Yamazaki, R. & Nakamura, T. 2006, *A&A*, 458, 7
- [153] Panaitescu, A. et al. 2006, *Mon. Not. Roy. Astron. Soc.*, 369, 2059
- [154] Gou, L. J. & Mészáros, P. 2007, *Astrophys. J.*, 668, 392
- [155] Fan, Y. et al. 2007, *Mon. Not. Roy. Astron. Soc.*, 384, 1483
- [156] Burrows, D. N. et al. 2005, *Science*, 309, 1833
- [157] Chincarini, G. et al. 2007, *Astrophys. J.*, 671, 1903
- [158] Falcone, A. D. et al., 2007, *Astrophys. J.*, 671, 1921
- [159] Falcone, A. D. et al., 2006, *Astrophys. J.*, 641, 1010
- [160] Liang, E. W. et al. 2006, *Astrophys. J.*, 646, 351
- [161] Wang, X.-Y., Li, Z., Mészáros, P. 2006, *Astrophys. J.*, 641, L89
- [162] Primack, J. R. et al. 1999, *APh*, 11, 93
- [163] Stecker, F. W., Malkan M. A. & Scully S. T. 2006., *Astrophys. J.*, 648, 774
- [164] Cheng, L. X., & Cheng, K. S. 1996, *Astrophys. J.*, 459, L79
- [165] Dai, Z. G., Lu, T. 2002, *Astrophys. J.*, 580, 1013
- [166] Wang, X. Y., Cheng, K. S., Dai, Z. G., Lu, T. 2004, *Astrophys. J.*, 604, 306
- [167] Plaga, R. 1995, *Nature*, 374, 430
- [168] Gehrels, N. et al. 2005, *Nature*, 437, 851
- [169] Fox, D. B. et al. 2005, *Nature*, 437, 845
- [170] Barthelmy, S. D. et al. 2005, *Nature*, 438, 994
- [171] Berger, E. et al. 2005, *Nature*, 438, 988
- [172] Bloom, J. S. et al. 2006, *Astrophys. J.*, 638, 354
- [173] Gehrels, N. et al. 2006, *Nature*, 444, 1044
- [174] Zhang, B. et al. 2007, *Astrophys. J.*, 655, L25
- [175] Wang, X. Y., & Mészáros, P. 2006, *Astrophys. J.*, 643, L95
- [176] Waxman, E., Mészáros, P. & Campana, S., 2007, *Astrophys. J.*, 667, 351
- [177] E. Waxman 1995, *Phys. Rev. Lett.*, 75, 386
- [178] M. Vietri 1995, *Astrophys. J.*, 453, 883
- [179] C. D. Dermer 2002, *Astrophys. J.*, 574, 65
- [180] M. Vietri 1998, *Astrophys. J.*, 507, 40
- [181] C. D. Dermer and M. Humi 2001, *Astrophys. J.*, 479, 493
- [182] Razzaque, S., & Mészáros, P. 2006, *Astrophys. J.*, 650, 998
- [183] Abdo, A. A. et al. 2007, *Astrophys. J.*, 666, 361
- [184] J. P. Rachen and P. Mészáros 1998, *Phys. Rev. D*, 58, 123005
- [185] A. Atoyan and C. D. Dermer 2003, *Astrophys. J.*, 586, 79
- [186] C. D. Dermer and A. Atoyan 2004, *Astron. Ap.*, 418, L5
- [187] T. Totani 1999, *Astrophys. J.*, 511, 41
- [188] Fragile, P. C., Mathews, G. J., Poirier, J. & Totani, T. 2004, *APh*, 20, 591
- [189] X. Y. Wang, K. S. Cheng, Z. G. Dai and T. Lu 2005, *Astron. Ap.*, 439, 957
- [190] E. Waxman and P. Coppi 1996, *Astrophys. J.*, 464, L75

- [191] Ellis, J.R., Mavromatos, N.E., & Nanopoulos, D.V. 1992, Phys. Lett. B, 293, 37
- [192] Amelino-Camelia, G., Ellis, J.R., Mavromatos, N.E., & Nanopoulos, D.V. 1997, Int. J. Mod. Phys. A, 12, 607
- [193] Gambini, R. and Pullin, J. 1999, Phys. Rev. D, 59
- [194] Albert, J. et al. [MAGIC collaboration] 2008, Phys. Lett. B, in press
- [195] Scargle, J., Norris, J., & Bonnell, J. 2007, Astrophys. J., 673, 972
- [196] Pe'er, A., & Waxman, E. 2005, Astrophys. J., 633, 1018
- [197] Franceschini, A., Rodighiero, G., Vaccari, M. 2008, Astron. & Astrophys., 487, 837
- [198] Kowalski, M. & Mohr, A. 2007, Astropart. Phys., 27, 533
- [199] Achterberg, A. et al. 2008, Astrophys. J., 674, 357
- [200] Stamatikos, M. & Band, D. L. 2006, AIP Conf. Proc. 836, 599